Fast Three-Dimensional Analysis of Eddy Current in Litz Wire Using Integral Equation

Shingo Hiruma[1], Hajime Igarashi[1], *IEEE Member*

[1]Graduate School of Information Science and Technology, Hokkaido University, 060-0814 Sapporo, Japan.

Eddy current loss in a Litz wire which has three-dimensional structure is analyzed using the integral equation method considering the proximity effect. In the present method, each wire is modeled as a polygonal line. One-dimensional integral equation is solved for the dipole magnetization generated by the anti-parallel eddy currents in the wire. The discretized integral equation can effectively be solved using an iterative method solver to compute the eddy current distribution in the wire due to the proximity effect.

Index Terms— **Litz wire, complex permeability, integral equation, eddy current, proximity effect, two potential method**

I. Introduction

IT has become important to evaluate the eddy current losses in multi-turn coils and Litz wires used in the electric machines and devices because of increase in the driving frequency. The eddy current losses in the multi-turn coils and Litz wires are caused by the skin and proximity effects. When analyzing the eddy currents by finite element method (FEM), we have to discretize the wires into fine elements in order to consider these effects. Heavy computational burden is, therefore, required to solve the resulting FE equation.

A homogenization method for analysis of multi-turn coils and Litz wires have been proposed in Ref.[1]. In this method, the coil region is modeled as a uniform material which has the same macroscopic characteristic as the original coil. Because the element size does not have to be smaller than the skin depth when using this method, the computational time can be made extremely shorter than that of the conventional method. However, it remains to be difficult to analyze twisted or woven structures which Litz wires have because the homogenization method is formulated assuming for simplicity that wires are parallel to each other.

We propose here a fast computational method for three dimensional analyses of Litz wires and multi-turn coils. In this method, each wire is modeled as a polygonal line. The one-dimensional integral equation is solved for the dipole magnetizations perpendicular to the wire axis which are generated by the anti-parallel eddy currents due to the proximity effect. The integral equation can effectively be solved by the iterative method such as Jacobi and Gauss-Seidel methods. One of the advantages of this method is that it does not need to discretize wire cross section into elements because the eddy currents inside the wire are analytically evaluated. As the result, the number of the unknowns and the computational time can be considerably reduced in comparison with the conventional FEM. Moreover, we can apply this method to any wires with complicated structures like the Litz wire.

In this paper, it will be shown that the complex powers of a multi-turn coil computed by the present method agree well with those computed by the conventional FEM. By using two potentials method [2], this method can also be applied to the coil wound around a magnetic core. This method is also applied to the analysis of three different wire models, that is, parallel wires, multiple strands, and rope lay, where the second and third models correspond to the Litz wire. It will be shown that the Litz wire models have smaller eddy current losses in comparison with the parallel wires.

II. Formulation

A. Complex permeability

Let us consider an isolated round wire, radius a, conductivity σ, relative permeability μ, immersed in a time-harmonic magnetic field of angular frequency ω. The curvature of the wire is assumed to be negligible so that the field is two dimensional. Then the eddy currents and corresponding dipole fields due to the proximity effect can be obtained by analytically solving the two-dimensional Helmholtz equation. The wire has diamagnetic property due to the anti-parallel eddy currents flowing along the wire. This property can be represented by introducing the complex permeability $\dot{\mu}$ given by [1]

$$\dot{\mu} = \mu_0 \frac{J_1(z)}{zJ_1'(z)} \tag{1}$$

where $z = a\sqrt{-j\omega\sigma\mu}$ and J_1 is the first-order Bessel function.

B. Integral equation

Now we consider a bundle of round wires along which carry alternating currents. The eddy current losses in the wire due to the skin and proximity effects can be separately determined because of the orthogonality between them [3]. The former can easily be computed by the analytical method. The anti-parallel eddy currents due to the proximity effect in a wire are induced by the alternating magnetic field generated by the currents carried by the surrounding wires. The eddy current distribution in the wires has to be determined self-consistently. To do so, we

Manuscript received November 19, 2016; revised May 15, 2015 and June 1, 2015; accepted July 1, 2015. Date of publication July 10, 2015; date of current version July 31, 2015. (Dates will be inserted by IEEE; "published" is the date the accepted preprint is posted on IEEE Xplore®; "current version" is the date the typeset version is posted on Xplore®). Corresponding author: H. Igarashi (e-mail: igarashi@ssi.ist.hokudai.ac.jp).

Digital Object Identifier (inserted by IEEE).

employ the complex permeability (1) assuming that the wire cross-sectional radius is much smaller than the curvature radius. Then, we consider the complex magnetization vector $\boldsymbol{M}$ perpendicular to the wire axis which is generated by the anti-parallel eddy currents. We assume that $\boldsymbol{M}$ is constant in the cross section of the wire, and it has one-dimensional distribution along the wire. The relation between $\boldsymbol{M}$ and the magnetic field $\boldsymbol{H}$ perpendicular to the wire is given by $\boldsymbol{M} = (\dot{\mu}_r - 1)\boldsymbol{H}$. The magnetic field $\boldsymbol{H}$ is composed of $\boldsymbol{H_0}$ generated by external currents and component due to the complex magnetization $\boldsymbol{M}$ distributed along the wire. Then, we obtain the following one-dimensional integral equation for $\boldsymbol{M}$:

$$\frac{\boldsymbol{M}(\boldsymbol{x})}{\dot{\mu}_r - 1} = \boldsymbol{\tau} \times \left[\left(\int_{\Omega_c} \mathcal{G}\boldsymbol{M} dv' + \boldsymbol{H}_0(\boldsymbol{x}) \right) \times \boldsymbol{\tau} \right] \tag{2a}$$

$$\mathcal{G}\boldsymbol{M} = -\frac{1}{4\pi}\left[\frac{\boldsymbol{M}(\boldsymbol{x}')}{R^3} - 3\frac{(\boldsymbol{M}(\boldsymbol{x}')\cdot \boldsymbol{R})\boldsymbol{R}}{R^5} \right] \tag{2b}$$

which is a natural extension of the magnetostatic integral equation [4], where Ω_c is the domain where the magnetization $\boldsymbol{M}$ exists, $\boldsymbol{x}$ and $\boldsymbol{x}$' are the observation and source points in Ω_c, $\boldsymbol{\tau}$ is the tangential unit vector parallel to the wire at $\boldsymbol{x}$, $\boldsymbol{R} = \boldsymbol{x} - \boldsymbol{x}'$, and $R = |\boldsymbol{R}|$. The external magnetic field $\boldsymbol{H_0}$ can be calculated by Biot Savart's law.

Discretizing the wire into line segments as shown in Fig.1, we obtain the discretized form of the integral equation as

$$\frac{\boldsymbol{M}_i}{\dot{\mu}_r - 1} = \boldsymbol{\tau}_i \times \left[\left(\sum_j \int_{\Omega_{cj}} (\mathcal{G}\boldsymbol{M})_{ij} dv' + \boldsymbol{H}_{0i} \right) \times \boldsymbol{\tau}_i \right] \tag{3a}$$

$$(\mathcal{G}\boldsymbol{M})_{ij} = -\frac{1}{4\pi}\left[\frac{\boldsymbol{M}_j}{{R_i}^3} - 3\frac{(\boldsymbol{M}_j \cdot \boldsymbol{R}_i)\boldsymbol{R}_i}{{R_i}^5} \right] \tag{3b}$$

where $\boldsymbol{R}_i = \boldsymbol{x}_i - \boldsymbol{x}'$, $R_i = |\boldsymbol{R}_i|$, $\boldsymbol{x}_i$ is the center of the i-th line segment, and $\boldsymbol{\tau}_i$ is the tangential unit vector of the i-th line segment. The domain Ω_{cj} is now a cylinder of the height l_i and the radius a. Note that we do not need to discretize the wire cross section into elements. If $i = j$, the integration can be analytically evaluated as

$$\begin{aligned} \int_{\Omega_{ci}} (\mathcal{G}\boldsymbol{M})_{ii} dv' &= -\frac{\boldsymbol{M}_i}{4\pi}\int_0^{\frac{l_i}{2}} dz' \int_0^a dr' \left(\frac{4\pi r'}{(r'^2 + z'^2)^{3/2}} - \frac{3\cdot 2\pi r'^3}{(r'^2 + z'^2)^{5/2}} \right) \\ &= -\frac{\boldsymbol{M}_i}{2}\frac{l_i}{\sqrt{4a^2 + {l_i}^2}} \end{aligned} \tag{4}$$

Otherwise the integration is computed numerically. If the segments are adjacent to one another, the integration (3) can be nearly singular. In this case, the accuracy of the numerical integration would significantly be deteriorated. To overcome this difficulty, we apply Log-L1 transformation [5] and DE formula [6] to the integration. If the segments are far apart, the volume integration is approximated to the line integration along the line segment in order to reduce the computational time.

The integral equations obtained in this manner lead to a dense

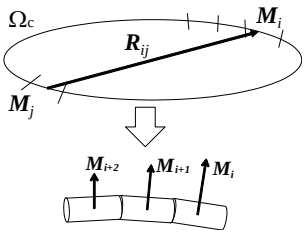

Fig.1. Wire model. The unknowns $\boldsymbol{M}_i$ are assigned to each line segment.

matrix system. It would take long time to solve the equation when we use direct methods such as the LU decomposition. Therefore, we use the iterative methods such as Jacobi and Gauss-Seidel method to solve the equation.

C. Computation of complex power

We first consider the current-input problem. The complex power of the wire can be represented as [1]

$$\frac{VI^*}{2} = \frac{j\omega}{2}\int_{\Omega_c} \boldsymbol{A}\cdot\boldsymbol{J}^* dv + \frac{R_0 z J_0(z)}{4J_1(z)}|I|^2 \tag{5}$$

where I and $\boldsymbol{J}$ are the total current and corresponding current density carried by each wire, and R_0 is the DC resistance of the wire, * represents complex conjugate and Ω_c is the wire region. In the evaluation of the first term in (5), $\boldsymbol{J}$ is assumed to be uniform in the wire cross section for simplicity. The first term in (5) includes stored magnetic power and power relevant to the proximity effect, while the second term represents the power relevant to the skin effect. When evaluating the integration, the vector potential is assumed to be constant in the line segment.

The vector potential in (5) is computed from

$$\boldsymbol{A} = \frac{\mu_0}{4\pi}\int_{\Omega_c} \frac{\boldsymbol{M}(\boldsymbol{x}')\times\boldsymbol{R}}{R^3} dv' + \frac{\mu_0}{4\pi}\int_{\Omega_c} \frac{\boldsymbol{J}(\boldsymbol{x}')}{R} dv' \tag{6}$$

After discretization, the first term (6) cancels out, if $i = j$. In this case, the contribution from the second term to the complex power (5) is represented as [7]

$$\frac{j\omega}{2}\int_{\Omega_{ci}} \boldsymbol{A}_i \cdot \boldsymbol{J}^* dv = \frac{j\omega}{2} L_i |I|^2 \tag{7}$$

$$L_i = \frac{\mu_0}{2\pi}\left(l_i \log\left(\frac{l_i + \sqrt{l_i^2 + a^2}}{a} \right) - \sqrt{l_i^2 + a^2} + a \right) + \frac{\mu_0 l_i}{8\pi} \tag{8}$$

Because the integration becomes nearly singular for the adjacent segments, the same technique mentioned above is employed.

Note that the proximity and skin effects are considered by introducing $\dot{\mu}$ and the second term in (5), respectively. For this reason, we can obtain the eddy currents by magnetostatic analysis. If there are other conductors, we have to modify (2) to include the eddy current terms.

D. Treatment of magnetic core

When magnetic core exists near the coil, the magnetic field generated by the magnetization in the core has to be also considered. Hence, we do not know $\boldsymbol{H}_0$ a priori in (2). To

determine the magnetic fields in a consistent way, we use here the two potentials method [2]. In this method, the analytical domain is divided into two sub-domains, total potential sub-domain Ω_t and reduced potential sub-domain Ω_r, as shown in Fig.2. The magnetic core exists in Ω_t, and the coils exist in Ω_r. The boundary of these sub-domains is denoted by Γ_{tr}. The magnetic field generated by the current in Ω_r is computed by the Biot-Savart law. In each domain, the following equations based on A method

$$\mathrm{rot}\,\nu\mathrm{rot}\boldsymbol{A}_t + j\omega\sigma\boldsymbol{A}_t = 0, \quad in \ \ \Omega_t \tag{9a}$$

$$\mathrm{rot}\,\nu_0\mathrm{rot}\boldsymbol{A}_r = 0, \quad in \ \ \Omega_r \tag{9b}$$

are solved using FEM. Then the following boundary conditions are imposed on Γ_{tr}:

$$\boldsymbol{A}_t \times \boldsymbol{n} = (\boldsymbol{A}_r + \boldsymbol{A}_s) \times \boldsymbol{n} \tag{10a}$$

$$\boldsymbol{H}_t \times \boldsymbol{n} = (\boldsymbol{H}_r + \boldsymbol{H}_s) \times \boldsymbol{n} \tag{10b}$$

where $\boldsymbol{H}_t = \nu\mathrm{rot}\boldsymbol{A}_t$, $\boldsymbol{H}_r = \nu\mathrm{rot}\boldsymbol{A}_r$, $\boldsymbol{H}_s$ and $\boldsymbol{A}_s$ are the magnetic field and magnetic vector potential on Γ_{tr} generated by the source currents.

In this method, the magnetic field in Ω_r is assumed to be generated by the magnetized magnetic core. Therefore, by adding the magnetic field $\boldsymbol{H}_r$ to the magnetic field $\boldsymbol{H}_0$ in (2), we can take account of the effect of the magnetic core. Then the magnetic field is modified to

$$\boldsymbol{H}' = \boldsymbol{H}_0 + \boldsymbol{H}_r \tag{11}$$

Similarly, the vector potential is modified to

$$\boldsymbol{A}' = \boldsymbol{A} + \boldsymbol{A}_r \tag{12}$$

The distribution of the magnetic dipole obtained by the integral equation also changes the magnetic field. In order to determine the fields self-consistently, eqs. (2) and (9) are solved alternatively.

E. Voltage-input problem

In the above-mentioned formulation, we consider the current-input problem where the same currents are assumed in all the wires although the currents would differ from each other in the actual Litz wires. Thus, we here consider the voltage-input problem. In this problem, the voltage at the terminals of each wire is set to a given voltage V. Because the integral equation cannot be solved if $\boldsymbol{J}$ is not given, we employ the following iterative method. First, the initial currents are assumed to each wire, and a system of the integral equations is solved. Then the impedance of each wire is evaluated from

$$Z_i = \frac{2P_i}{|I_i|^2} \tag{13}$$

where P_i the complex power of i-th wire. Then the currents are redistributed by AC Ohm's law:

$$I_i^{new} = \frac{V}{Z_i} \tag{14}$$

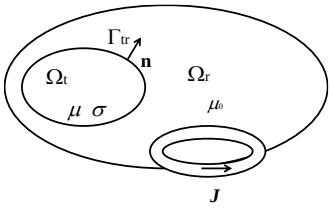

Fig.2. Domains in the two potentials method

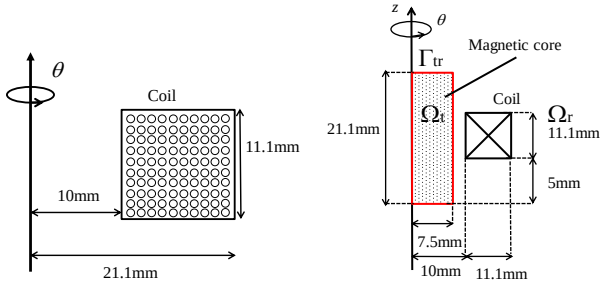

Fig.3. 100-turn coil and 100-turn coil wound around a magnetic core

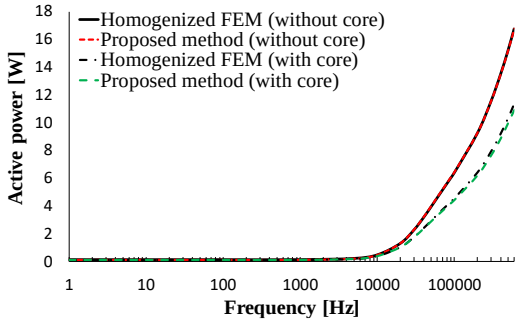

Fig.4. Frequency characteristic of the active powers obtained by the FEM and proposed method

The integral equations including the new currents are solved again for $\boldsymbol{M}$. After the iteration, we can determine the currents I_i for given V self-consistently.

III. NUMERICAL RESULTS

A. Validation on a coil composed of parallel wires

We apply the proposed method and conventional FEM based on the homogenization method described in [1] to the 100-turn coil model shown in Fig.3. The radius of the wire is 0.5 mm, and the conductivity of the wire is 5.76×10^7 S/m. In discretization, each wire is subdivided into 100 line segments with equal length. Fig.4 shows the frequency characteristic of the complex powers obtained by both methods. We can see that the active powers are in good agreement from low frequency to high frequency. The maximum difference is 3%.

We also apply the proposed method to the analysis of the 100-turn coil model wound around a magnetic core. The relative permeability of the magnetic core is 1000. Three iterations to solve (2) and (9) are required to obtain the convergent solution. The frequency characteristic of the active powers is shown in Fig.4. We again see that the results obtained by proposed method and FEM are in good agreement. The maximum difference is 5%.

B. Analysis of Litz wire model

We apply the proposed method to the analysis of three wire models, that is, parallel, multiple strands and rope lay. Each

model consists of 49 wires, radius 0.15 mm, pitch 15 mm and conductivity 5.76×10^7 S/m. The wires are assumed to form a straight Litz wire, one period of which is analyzed. In the parallel strands, wires are not twisted and bundled up. Wires are twisted in the multiple strands, while the groups of twisted wires are twisted in the rope lay [8] as shown in Fig.5. The total number of unknowns is 2,450.

Assuming that a net current, 1 A, is imposed to each wire, the active powers in the three types of strands are computed. The results are plotted against frequency in Fig.6. We can see the active power of the parallel wires is the highest, while other two powers have no significant differences and are lower than that for the parallel wires. This result is consistent with the result obtained by conventional FEM with "Earth simulator", highly parallel supercomputer [8]. These results are due to the fact that the twist of wires reduces the proximity effect. This tendency can be verified when we see the eddy current distributions in the parallel and rope lay models shown in Fig.7.

The resultant active powers for the voltage-input problem mentioned in III.*E* are plotted against frequency in Fig 8. We can see that the active power in the parallel strands is the highest in low frequency because the DC resistance of the parallel model is the lowest of the three model. The active powers decrease as frequency becomes higher because the impedance of the wire increases due to the proximity effect.

C. Computational time

The dependence of the computational time and memory usage of the proposed method on the number of wires are shown in Fig.9, where each wire is discretized into 50 segments. We can see that the computational time increases almost linearly, while the memory usage increases quadratically. It is because the equation includes the dense matrix.

IV. CONCLUSION

In this paper, we have proposed a novel method based on the one-dimensional integral equation for the magnetization generated by eddy currents due to the proximity effect. By using this method, we can easily model complicated windings because we do not need to discretize the wire cross section and the insulator between the coils into elements. It has been shown that the active powers computed by the proposed method are in good agreement with those computed by the conventional FEM which needs fine discretization of wire and insulators. It has been numerically shown that the eddy current losses in the Litz wire models are smaller in comparison with the parallel strands.

REFERENCES

[1] H. Igarashi, "Semi-Analytical Approach for Finite Element Analysis of Multi-turn Coil Considering Skin and Proximity Effects," *IEEE Trans. Magn*., vol.53, no.1, 7400107, 2017.

[2] A. Kameari, "Regularization on Ill-posed Source Terms in FEM Computation Using Two Magnetic Vector Potentials," *IEEE Trans. Magn*., vol. 40, no. 2, pp. 1310-1313, 2004.

[3] J. A. Ferreira, "Improved Analytical Modeling of Conductive Losses in Magnetic Components," *IEEE Trans. Power Electronics*, vol.9, no.1, 1994, pp.127-131.

[4] P. P. Silvester, et al., *Finite Elements for Electrical Engineers*, 1996

[5] K. Hayami, "High Precision Numerical Integration Methods For 3-D Boundary Element Analysis," *IEEE Trans. Magn*., vol. 26, no. 2, pp 603-606, 1990.

[6] H. Takahashi, M. Mori, "Double Exponential Formulas for Numerical Integration," *Publ. RIMS*, Kyoto Univ., September 1974, pp. 721-741.

[7] E. B. Rosa, The Self And Mutual Inductances Of Linear Conductors, pp. 301-344, 1908.

[8] Y. Kawase, et al., "3-D Finite Element Analysis of Eddy Current Loss in Stranded Wire Coil," Proc. ISEF2015, 2015.

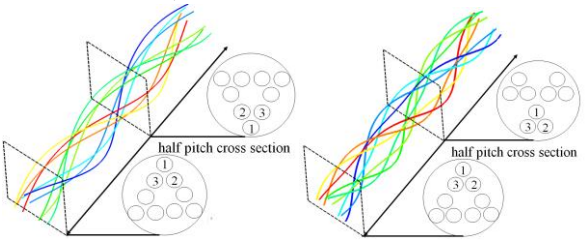

Fig.5. Difference between the multiple strands (left) and rope lay (right)

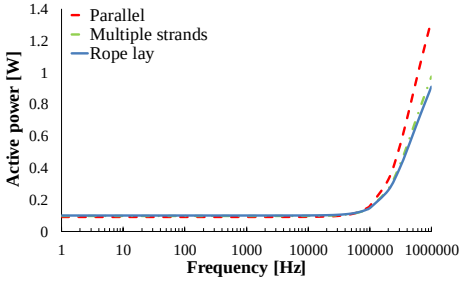

Fig.6. Frequency characteristic of active powers for three models when unit current is imposed

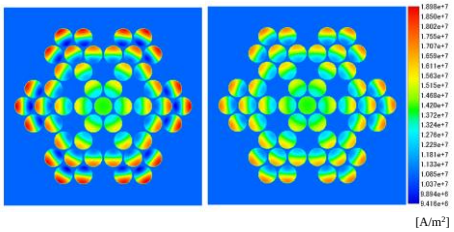

Fig.7. Distribution of eddy current density in parallel (left) and rope lay (right) models at 100 kHz. The eddy currents are computed as follows: the external magnetic field $\boldsymbol{H}$ which is applied to the wire can be computed from $\boldsymbol{H}=\boldsymbol{M}(\dot{\mu}_{\mathrm{r}}+1)/2(\dot{\mu}_{\mathrm{r}}-1)$. The eddy currents in the wire immersed in $\boldsymbol{H}$ is then determined analytically as shown in Ref.[1].

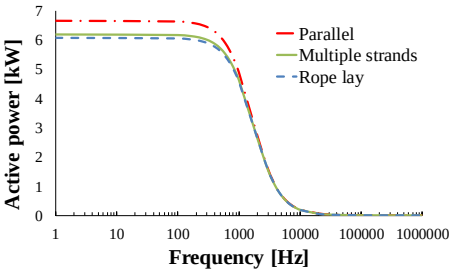

Fig.8. Frequency characteristic of active powers for three models when unit voltage is imposed

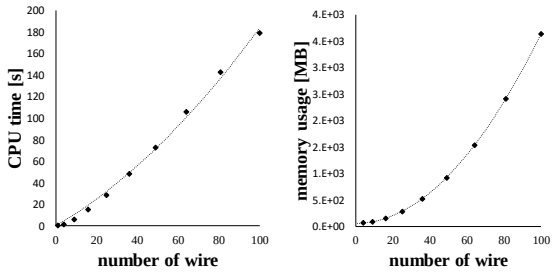

Fig.9. Computational time (left) and memory usage (right)